Gas monitoring in RPC by means of non-invasive plasma coated POF sensors

PUBLISHED BY IOP PUBLISHING FOR SISSA MEDIALAB

RECEIVED: *July 30, 2012*
ACCEPTED: *October 30, 2012*
PUBLISHED: *December 7, 2012*

SPECIAL ISSUE ON RESISTIVE PLATE CHAMBERS AND RELATED DETECTORS RPC2012

Gas monitoring in RPC by means of non-invasive plasma coated POF sensors

S. Grassini,[a,1] M. Ishtaiwi,[b] M. Parvis,[b] L. Benussi,[c] S. Bianco,[c] S. Colafranceschi[c] and D. Piccolo[c]

[a] *Dipartimento di Scienza Applicata e Tecnologia, Politecnico di Torino, Corso Duca degli Abruzzi 24 Torino, Italy*
[b] *Dipartimento di Elettronica e Telecomunicazioni, Politecnico di Torino, Corso Duca degli Abruzzi 24 Torino, Italy*
[c] *Laboratori Nazionali di Frascati dell'INFN, v. E. Fermi 40, Frascati 00044, Italy*

E-mail: sabrina.grassini@polito.it

ABSTRACT: Resistive Plate Counters (RPC) are employed as muon detectors in many high-rate high-energy physics experiments, such as the Compact Muon Solenoid (CMS) experiment currently under way in the Large Hadron Collider (LHC) accelerator at the European Center for Nuclear Research (CERN). A gas mixture containing $C_2H_2F_4$, $i-C_4H_{10}$ and SF_6 is recirculated inside the RPCs during their use and subjected to degradation due to the production of fluoride ions which limits the sensitivity of the RPCs. This paper describes a new sensor that is able to detect low concentrations of fluoride ions in gas mixtures. The sensor is made of a plastic optic fiber (POF) which is made sensitive to F^- gaseous ions by means of a thin layer of a glass-*like* material, deposited via plasma onto the fiber core. The F^- ions attack the glass-*like* film and alter the transmission capability of the fiber so that the detection simply requires a LED and a photodiode. The sensor exploits a cumulative response which makes it suitable for direct estimation of the total exposure to the F^- ions, thus providing a tool that can be used to tune the maintenance of the gas filters. The glass-*like* film is deposited by means of plasma enhanced chemical vapor deposition (PECVD) of organosilicons monomers, which allows the deposition to be performed a low temperature in order to avoid damaging the fiber core.

KEYWORDS: Gaseous detectors; Gas systems and purification; Resistive-plate chambers

[1] Corresponding author.

doi:10.1088/1748-0221/7/12/P12006

2012 JINST 7 P12006

Contents

2012 JINST 7 P12006

1 Introduction

Resistive Plate Counter (RPC) [1] detectors are widely used in nuclear and particle physics for the detection and timing of muon particles. The adoption of an F-based gas mixture as an active medium in RPCs makes it necessary to understand what damage it can have on RPC materials, what contaminants are produced in the recirculation systems which are the effects effects connected to their use in high-radiation areas. The results of a study on optical sensors for fluorine contaminants are reported hereafter. The study to establish a possible application of such optical sensors in the RPC muon detector [2] of the Compact Muon Solenoid (CMS) experiment [3] in the Large Hadron Collider (LHC) at the European Center for Nuclear Research (CERN) in Geneva (Switzerland). The RPCs which are employed in the CMS are composed of two bakelite plates kept 2 mm apart by means of spacers. The plates are maintained at a voltage difference of about 9 kV in order to obtain an electric field of about 4.5 kV/mm between the plates. The space between the plates is filled with an insulating gas whose ionization, connected to the passage of a charged particle, is used for particle detection. The gas is a mixture of 96.2% of $C_2H_2F_4$, 3.5% of $i-C_4H_{10}$ and 0.3% SF_6 and is maintained at a fixed relative humidity of 45%. A closed-loop recirculation system is used because of the large volume and cost of the gas being used. During RPC operation, the gas mixture may be polluted by contaminants that increase the RPC dark current. One of the identified contaminants, which is critical for its reactivity and difficult to detect, is hydrogen fluoride (HF).

The average HF production of one CMS RPC chamber has been estimated to be about 25 μmol/h, which corresponds to concentrations, in the absence of filters, of some parts per million [4, 5]. For this reason, 90% of the gas mixture is recirculated and purified by 3 gas filters, while 10%-20% of fresh gas is injected into the loop, thus reducing the HF concentration to 0.1 μmol/h.

The concentration of contaminants is monitored by means of electrochemical F^- sensors and gas chromatography. Gas sampling points are located before and after each filter. The sampling points make it possible to perform chemical samplings in a lithium hydroxide solution, whose composition is determined at fixed intervals by means of chemical analyses.

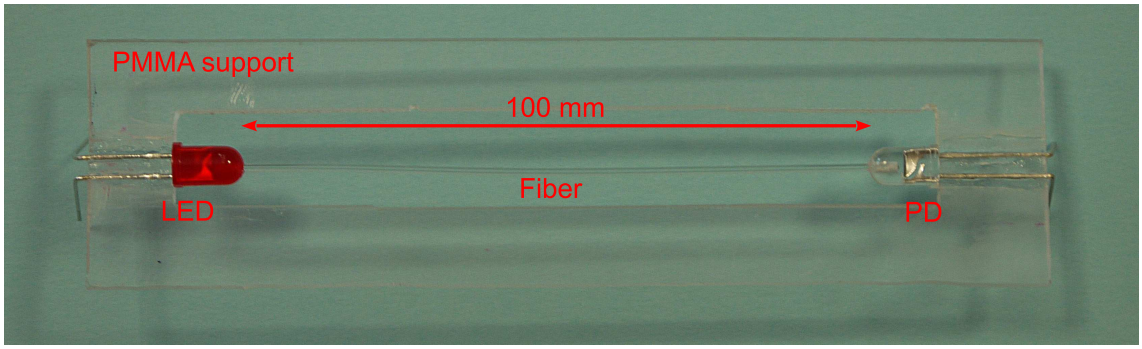

Figure 1. Sensor assembly with LED, fiber and PD.

Commercially available sensors for fluoride ion detection (e.g. galvanic-type sensors that are based on MnO_2 gas-diffusion electrodes [6]) have a measuring range of $10 - 20$ ppm, which is too high for this kind of measurement. These commercial Hydrogen Fluoride sensors (e.g. from CEA Instruments Inc, GasDetectors USA) are designed for personal safety and have costs in excess of 500$ per unit so that their massive use for a complete RPC monitoring is not feasible.

More sensitive sensors, such as tin dioxide and Al-doped graphene based devices [7–9], have been proposed to detect hydrogen fluoride traces at part-per-billion concentration, but they all have a higher cost.

Intrinsic sensors based on Plastic Optical Fibers (POFs) made of poly-methyl-methacrylate (PMMA) [10, 11] could be an interesting alternative, provided they can be made sensitive to fluoride ions. The use of POFs for sensing applications is rapidly growing [12–14] because of the cost-effectiveness of the POFs and the easiness of use connected to their large diameters (0.25 mm $- 1$ mm), which permit simple and cheap plastic connectors to be used while still maintaining a good optical coupling [15]. Fiber optics can be used to develop intrinsic sensors, thanks to several different principles (fiber grating, scintillation, light attenuation changes due to pollutant absorbtion in the core, light losses due to fiber bending, etc... [16, 17]). However, POFs offer the advantage of having a remarkable evanescent field, which extends outside the core and which can be used to develop sensors based on the propagation loss change that occurs due to the interaction of the evanescent field with the surrounding media.

2 Sensor design

A fiber based sensor that exploits the interaction of the evanescent field with the surrounding environment can easily be arranged with a structure composed of a light emitting diode, an optic fiber and a photodiode, as shown in figure 1.

The fiber has a length of about 10 cm. The used LED (Kingbright L-53SRD-G) emits in the visible red region (wavelength 635 nm–680 nm) and has been selected since PMMA has a stable attenuation value in the red region [22] when exposed to radiations. A wide band photodiode (Osram SFH 213) is also employed.

Both LED and PD cupolas are drilled with 1 mm holes; the fiber is inserted into the holes and bonded to the components using liquid PMMA. The fiber is then cured in an oven at 60 °C for three days to ensure complete polymerization of the liquid PMMA. Finally, the assembly is bonded to a PVC support so that the fiber is retained in a fixed position.

2012 JINST 7 P12006

In order to exploit the use of the evanescent field, the POF cladding must be removed and the core exposed so that the sensitive film can directly interact with the evanescent field.

Commercially available fibers commonly used for telecommunication purposes, costing about 1$ per meter, can be employed to develop the sensor. These fibers are step-index, highly multi-mode POFs with a 0.98 mm diameter PMMA core, surrounded by a 0.01 mm fluoropolymer cladding.

The cladding can be removed either by means of a mechanical process or by means of a chemical process. The mechanical approach is difficult to carry out without damaging the core, which is composed of PMMA that is a relatively soft material; on the other hand, a pure chemical approach is not feasible since the long exposure to the solvent that is necessary to obtain the complete dissolution of the fluoropolymer would damage the core. For this reason,the authors have employed a mixed chemico-mechanical approach. Initially, the fiber is dipped into ethylacetate for 40 s, so that the fluoropolymer is attacked, then the cladding is stripped using a soft paper towel, which is able to remove the fluoropolymer without damaging the core.

Once the cladding has been removed, the sensitive film must be deposited using a low temperature process, since the PMMA core is damaged at temperature higher than 80 °C. A good solution, which also allows a precise control of the layer structure to be obtained, is the use of low pressure plasma treatments or 'cold plasmas'. Plasma Enhanced Chemical Vapor Deposition (PECVD) can be used to develop very sensitive sensors [18]. PECVD modifies the fiber surface properties either by grafting different functional groups, or by depositing thin films, whose physico-chemical and optical properties can be changed over a broad range simply by making a proper selection of the experimental parameters.

The critical aspect in the design of a POF sensor that exploits the evanescent field and its interaction with the surrounding media in order to achieve sensitivity to the quantity of interest concerns the selection of the sensitive film. The film that has to be deposited on the fiber core must be capable of reacting with the sensed quantity of interest with a reaction which alters the capability of the fiber of transmitting the light. In addition, to achieve the required selectivity, the film must have a minimal reacting capability with respect to other quantities present in the surrounding environment, which could also affect the light transmission.

This selectivity can easily been obtained in the case of fluoride ions by employing a glass-*like* thin film. Glass has a higher refractive index than the PMMA and thus affects light transmission to a great extent. It is attacked by the F^- ions and is almost unaffected by other quantities. Two problems arise: first the direct deposition of glass onto the fiber is impossible since the melting temperature of glass is much higher than the melting temperature of PMMA; second, a careful control of the glass thickness is fundamental to obtain good interaction with the evanescent field. It is important to note that the reaction between glass and fluoride ions is not reversible and leads to the formation of silicon tetrafluoride (SiF_4):

$$SiO_2 + 4HF \Rightarrow SiF_4 + 2H_2O \tag{2.1}$$

The developed sensor shows intrinsic cumulative behavior, i.e., the sensor output is proportional to the integral of the exposure to the HF vapors. When coupled to conventional sensors for the detection of other contaminants, such as O_2, N_2, H_2O, the sensor will provide a direct measurement of the residual purifier lifetime. The cumulative mode of operation requires that the sensor should be discarded after use, thus dictating the need for a cheap product.

2012 JINST 7 P12006

The fiber can therefore be coated with an SiO_x film which has a very similar composition and amorphous structure to glass. SiO_x thin films with thicknesses of up to a few hundred nanometers can easily be deposited on the POF surface by means of PECVD starting from organosilicon monomers.

The plastic fibers were therefore treated in a plasma fed with tetraethoxysilane (TEOS), O_2 and Ar in different ratios. The plasma discharge was performed at a pressure of 5 Pa and with an input power of 50 W. The thickness of the deposited SiO_x film can be changed simply by varying the deposition time.

The PECVD reactor employed in this study consists of a stainless steel vacuum chamber connected to a turbomolecular pump backed up by a rotary pump. A 1 kW 13.56 MHz RF power generator connected through an impedance matching unit is used to ignite the discharge. A throttle valve and a pressure gauge permit the chamber pressure to be controlled. Four injection lines equipped with mass flow controllers permit quaternary discharge gas mixtures to be used. A separate controller is used for the injection of the film precursor vapor.

The fibers were processed onto the ground electrode at the floating temperature reached by the plasma, which was kept below 70°C, in order to avoid damaging the PMMA core. Thanks to the high conformability of the plasma discharge the entire surface exposed to the plasma can be coated, except for the point in contact with the ground electrode. The depositions were performed therefore in two steps, reversing the fiber half way to cover the entire surface thus obtaining a uniform thickness. In order to assess the conformability of the plasma discharge, some deposition experiments were performed onto Si patterned wafer specimens, which demonstrated the good homogeneity of the coating thickness (see figure 2). As an example, figure 2 shows a Field Emission Scanning Electron Microscope (FESEM) image of a deposited film, which has a structure that closely resembles the amorphous structure of glass. The figure shows how the thickness of a film with average thickness of 145 nm has a variability of no more than 20 nm between horizontal and vertical surfaces.

Finally, the LED, PD and the connections were painted with a black HF resistant paint to avoid problems due to the effect of environmental light and/or of the light which could travel from LED to the PD outside the fiber.

The described procedure allows one to obtain rather cheap assemblies, but has two main drawbacks. First, the initial transmission capability is closely connected to the position of the LED/PD holes, with respect to the cupola centers, and is also affected to a great extent by the polishing of the fiber ends. These problems could lead to rather different PD currents, even in the presence of a fixed LED current and, therefore, the PD conditioning circuit should have a variable gain to compensate for this variability. However, if all the measurements are scaled to the initial transmittance, the mounting effect can be rendered unimportant. The second, more important drawback is connected to the different expansion ratios of the fiber and the fiber support. This results in fiber stretching and/or bending, which can have an effect on the transmission capability of about 5% for temperature changes of 5 °C. This is not a problem in the RPC use, since the temperature is controlled and the temperature changes are usually lower than 1 °C; however, a new setup is currently being designed in which a different bonding solution is employed in order to reduce the effect of the changes in temperature.

2012 JINST 7 P12006

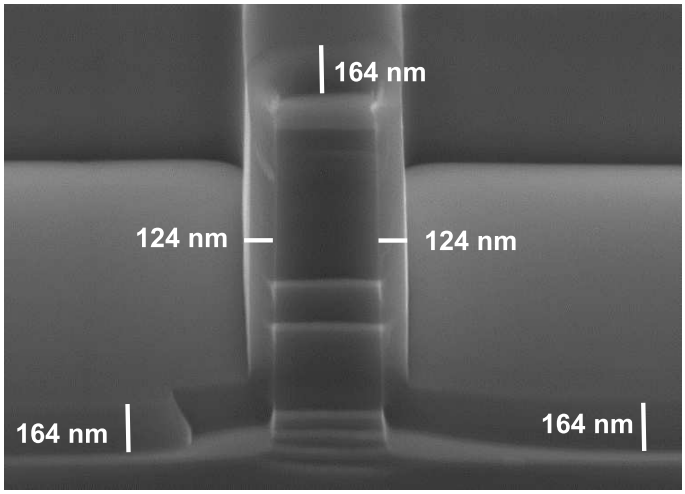

Figure 2. FESEM image of the cross-section of the SiO_x film deposited onto a Si patterned wafer. The coating thickness is quite homegeneous in the range of 124 nm to 164 nm demonstrating the good conformability of the plasma discharge.

3 Experimental results

3.1 Radiation effect

Since the sensors are designed to be employed in the presence of high-energy radiations, it is important to assess the behavior of the plastic fiber, the LED, and the PD when exposed to such radiations. Studies are in fact available regarding the behavior of glass fibers in the presence of radiation [19–21], but few results are available regarding plastic fibers [22]. In general, high energy radiations can produce fiber depolymerization that could reduce the transparency of the fiber, thus impairing the performance of the sensor. According to the results described in [22], the expected change is of about 1 dB/m for a PMMA fiber excited with a red wavelength and subjected to a dose of 100 Gy. This corresponds to an amplitude change of the order of 5% on a 10 cm long fiber in the same conditions, while negligible changes should be recorded for doses of the order of 1 Gy, which are the values expected in the fiber installation position for several months of CMS operation. To test this effect two sensor assemblies, one using a bare fiber and one with a fiber coated with a silver thin film, were installed and left in place for about six months in the Gamma Irradiation Facility (GIF) at CERN. The silver layer was chosen because it can easily be deposited via plasma, it can react with fluoride vapors, and it can lead to the formation silver fluoride (AgF) which, due to its yellow color, can alter the light transmittance of the fiber. This kind of coating was not used in the final sensors since it is sensitive to many other pollutants and provides limited sensitivity [14].

After this period, which corresponds to a dose of about 2 Gy, no changes in the transmission ratio were recorded on the bare fiber, while a small transmission reduction, of the order of 5%, was observed for the silver coated fiber, probably because of a slight tarnishing caused by the reaction between the silver film and the atmosphere.

3.2 Fiber coating

2012 JINST 7 P12006

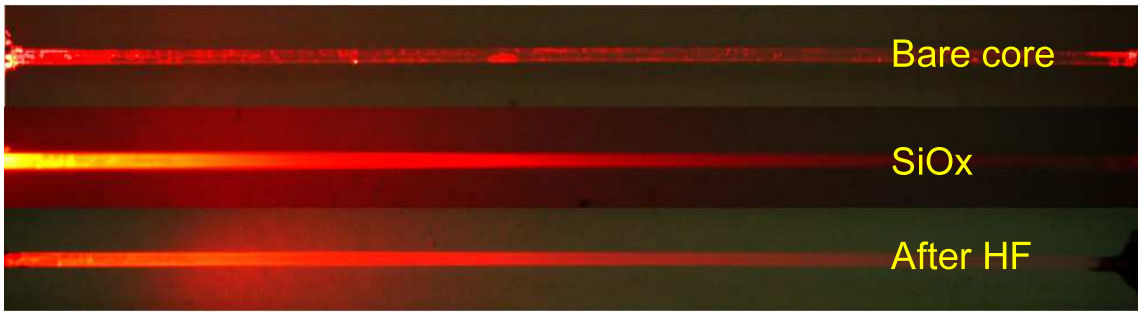

Figure 3. Example of dark field pictures of a fiber coated with a thick layer of SiO_x (400 nm). Top image: uncoated fiber; middle image: the SiO_x coated fiber; bottom image: SiO_x coated fiber after exposure to HF vapors.

When the fiber is coated according to the procedure described in the previous section, two parameters must be considered: the gas composition and the deposition time. The gas composition determines the nature of the coating, i.e. the organic/inorganic nature of the SiO_x layer. Since the objective is to obtain a layer with a high refractive index, a glass-*like* film is desired and this results in the deposition in an oxygen rich plasma in order to reduce the organic fraction of the film. The authors therefore employed a $TEOS : O_2 : Ar = 1 : 20 : 20$ sccm mixture, which allows one to obtain a mostly inorganic SiO_x film, as confirmed by the FTIR.

The deposition time determines the coating thickness: a too thin layer leads to an insufficient dispersive effect, while a too thick layer can reduce the received light to a very low value and produce a sensor with extremely low sensitivity since the fluoride attack cannot completely destroy the film.

An Si specimen was inserted into the plasma reactor along with the fiber to allow easy measurement of the film thickness by means of an FESEM. Figure 3 shows, as an example, dark field pictures of a fiber coated with a 400 nm thick SiO_x film obtained after a deposition time of 30 min. The top image shows the fiber core. The light dispersion is minimal and is due to the roughness of the fiber as a consequence of the cladding removal. The middle picture shows the same fiber after the SiO_x film deposition: the layer, which is quite thick, makes the fiber highly dispersive so that the light barely reaches the photodiode. The bottom image shows the fiber after exposure to HF vapors, as described in the following section. In the latter case, the fiber is less dispersive, but still barely any light reaches the photodiode, as the thick SiO_x is only partially attacked by the acid vapors. Figure 4 instead shows dark field pictures of a fiber coated with a 200 nm thick SiO_x film obtained after a deposition time of 15 min.

The top picture shows the bare fiber with a small slight dispersion, and is similar to the result of figure 3. The middle image shows the dispersion increase due to the 200 nm film, although less change can be observed than in the case of figure 3, since the layer is thinner. A small amount of light is still able to reach the end of the fiber. The bottom picture, taken after exposure to the HF vapors, shows degradation of the glass-*like* 200 nm film, which results in a reduced dispersion, so that the light at the end of the fiber significantly increases compared to the coated unexposed fiber. For these reasons, the POF sensor prototypes developed in this study have been coated with a 200 nm thick SiO_x film.

2012 JINST 7 P12006

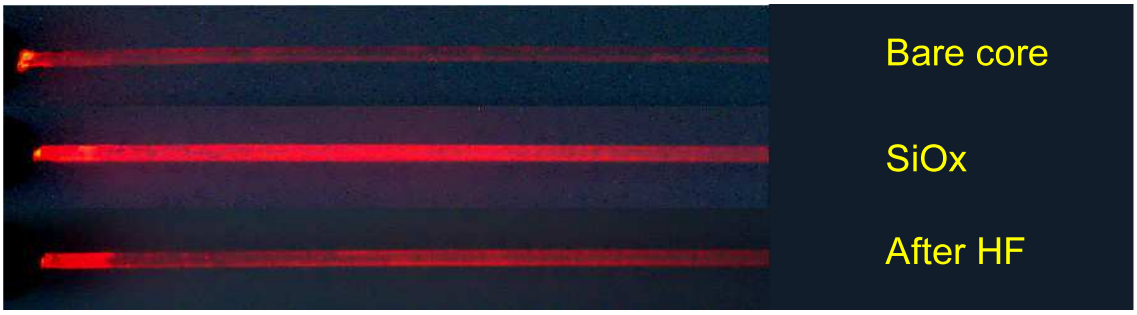

Figure 4. Example of dark field pictures of a fiber coated with a thin SiO_x film (200 nm). Top image: uncoated fiber, middle image: fiber after coating, bottom image: coated fiber after exposure to HF vapors.

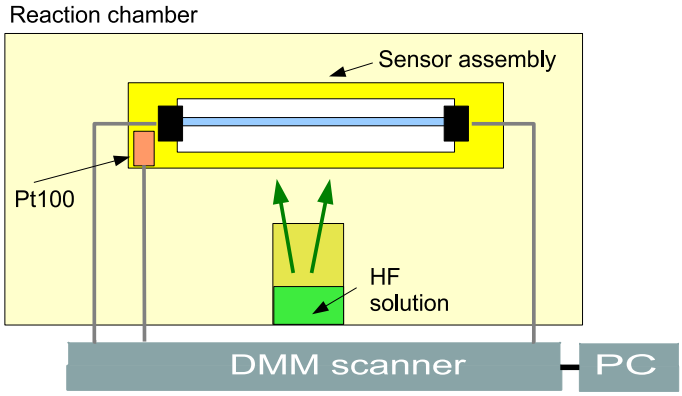

Figure 5. Block diagram of the measurement setup which comprises the sensor assembly, a T sensor ((RS Platinum Thin Film class A *Pt*100) a DMM-scanner and a PC connected to the scanner via IEEE488 interface. The reaction chamber is made of polytetrafluoroethylene (PTFE) which is HF-resistant. The HF vapors are generated by inserting a small PTFE bowl containing a calibrated solution of HF into the reaction chamber.

3.3 Exposure to HF

The effect of HF on the SiO_x coated POF sensor has been investigated by employing the measuring setup shown in figure 5. The sensor assembly is enclosed in a polytetrafluoroethylene (PTFE) chamber which can be sealed completely. A T sensor (RS Platinum Thin Film class A *Pt*100) is also inserted into the chamber and used to monitor the temperature. HF vapor generation is obtained by using a small PFTE bowl containing a few milliliters of HF solutions with different concentrations. This way it is possible to create HF vapors with different partial pressure by simply changing the concentration of the HF solution. The partial pressure can be computed using the Antoine equation [23] and the coefficients can be found either on the NIST web site [24] or computed from partial pressure experimental measurements [25].

The exposure tests were performed by employing a 40% in volume HF certified solution. The solution was diluted to 20% in volume, which corresponds to a partial pressure of about 700 Pa, at a temperature of about 25°C. All the tests were performed leaving the fiber in the bowl for some hours in clean air and then inserting the PTFE bowl with the HF solution into the chamber and leaving the measurement running until the fiber output reached a plateau.

2012 JINST 7 P12006

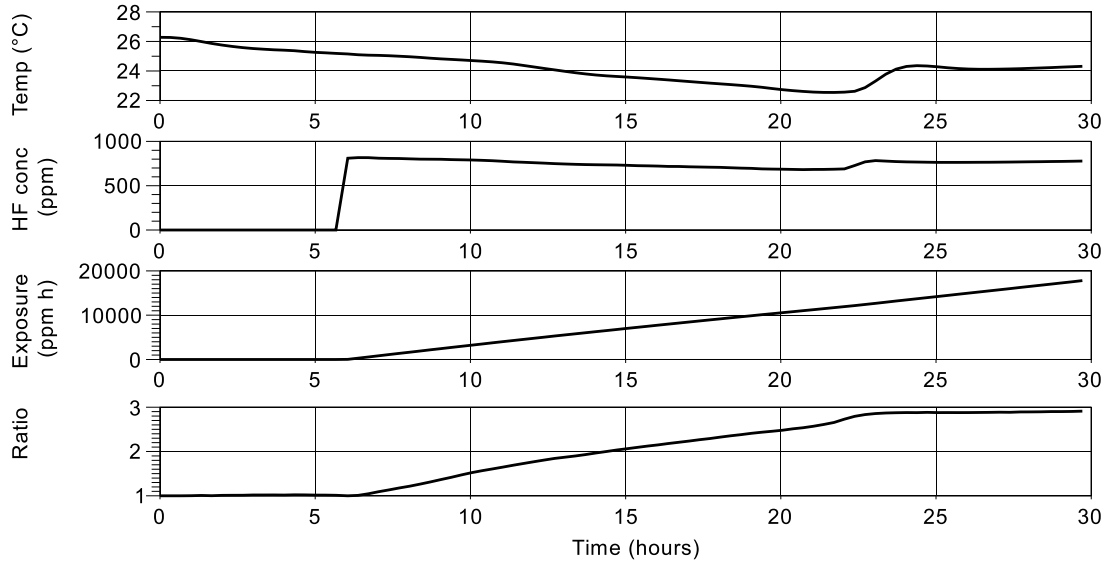

Figure 6. Coated fiber response to HF exposure. From top: Temperature during the test measured with the T sensor; HF vapor concentration computed according to the Antoine equation; exposure computed as the integral of the vapor concentration; fiber transmittance ratio normalized to its initial value. The test which lasted more than two days was conducted in a uncontrolled environment in which the temperature during the test changes in the range of 22 °C to 27 °C; only the first 30 hours are shown as the transmission ratio reaches a plateau after about 25 hours. The fiber has an output that follows the exposure until saturation, which appears when the transmission ratio increases about 3 times.

Figure 6 shows, as an example, the result of an exposure test. The figure shows the temperature measured by the T sensor, the HF vapor concentration computed using the Antoine equation, after the HF bowl had been inserted into the chamber after about five hours during which the fiber signal reached stability. The two lower traces show the exposure computed as the integral of the vapor concentration and the fiber transmittance ratio normalized to its initial value. The test, which lasted about two days, was conducted in an uncontrolled environment, in which the temperature during the test changed in the range of 22 °C to 27 °C. The picture shows the first 30 hours during which the fiber has an output that follows the exposure until saturation, which appears when the transmission ratio increases about 3 times. After about 25 hours, the transmission ratio reaches a plateau.

An FESEM analysis of the SiO_x film (figure 7) shows the film morphology after the HF attack. The SiO_x coated fiber surface can be observed on the left before HF exposure,while the images taken after exposure at different magnification levels, can be seen in the center and on the right. Before exposure, the SiO_x film appears smooth and homogeneous, while it is extensively corroded after exposure to the aggressive atmosphere and thus looses part of its dispersing capability.

Finally, figure 8 shows the exposure estimated from the fiber output using the equation:

$$E = k_f(R-1) \tag{3.1}$$

where R is the fiber transmittance normalized to its initial value and k_f is the transmittance sensitivity, identified on the basis of experimental data, which has a value of about 7000 $(\text{ppm}\cdot\text{hour})^{-1}$.

2012 JINST 7 P12006

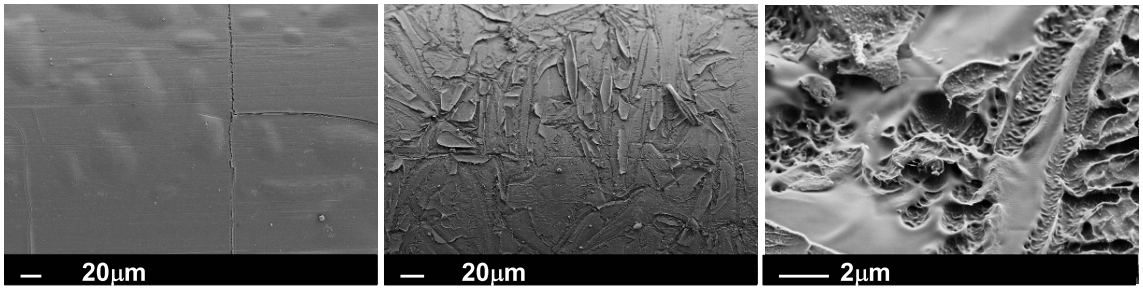

Figure 7. FESEM images of the coated fiber before (left) and after (center and right) exposure to the HF vapors.

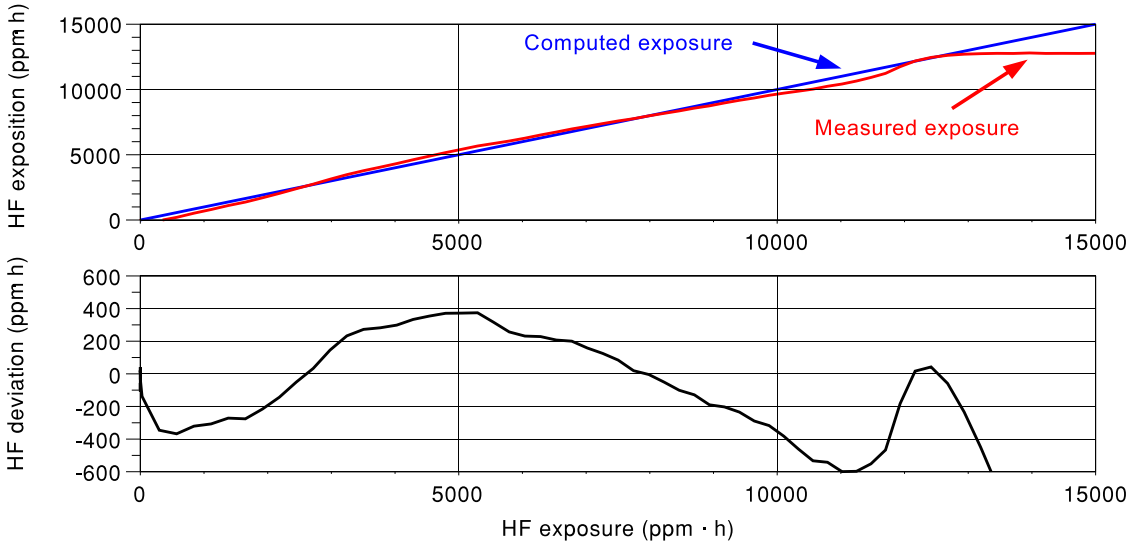

Figure 8. Exposure estimated on the basis of the sensor output and difference with respect to the expected value. The difference remains within 400 ppm · hour until the sensor reaches the end of life after exposure of about 10000 ppm · hour.

The blue line in the figure is the ideal expected response, while the red line is the measured response; the difference between the estimated and expected exposure can be observed at the botton. The difference remains within 400 ppm · hour until the sensor reaches the end of the life after exposure of about 10000 ppm · hour.

4 Conclusions

A new cumulative sensor prototype which can be used to monitor the presence of HF in gas mixtures employed in RPCs has been designed. The sensor, which can be obtained by coating a plastic optical fiber with a thin SiO_x layer deposited by means of PECVD, shows a high selectivity with respect to the fluoride ions and has a cost of the sensitive part of few dollars. The experiments described in this paper, have shown that the light transmitted by the fiber changes as soon as the SiO_x is attacked by HF vapors; in particular, changes of 3 times after exposition of 15000 ppm

2012 JINST 7 P12006

per, hour have been observed. The sensor has also been tested for operability in the presence of high-energy radiations and no changes have been observed when the sensor was exposed to a dose of about 2 Gy. This makes it possible to conclude that it could be employed in the RPC for longer periods than six months without any radiation-induced degradation. The sensor could be equipped either with a wireless battery-operated controller, to avoid wire connections, or with a standard acquisition system if electromagnetic interferences have to be avoided. The sensors are still sensitive to environmental conditions, which limits their accuracy and this is mainly due to the procedure adopted to mount the assembly. A new mounting structure is currently being designed in order to reduce this problem, however, the low cost of this sensor and its ability to work in the presence of high energy radiations make it a promising solution for large-scale, continuous monitoring for experiments employing a large number of RPCs, such as in the CMS site.

References

[1] R. Santonico and R. Cardarelli, *Development of resistive plate counters*, *Nucl. Instrum. Meth.* **187** (1981) 377.

[2] A. Colaleo et al., *First measurements of the performance of the barrel RPC system in CMS*, *Nucl. Instrum. Meth.* **A 609** (2009) 114.

[3] CMS collabroation, S. Chatrchyan et al., *The CMS experiment at the CERN LHC*, 2006 *JINST* **3** S08004.

[4] M. Abbrescia et al., *Results about HF production and bakelite analysis for the CMS resistive plate chambers*, *Nucl. Instrum. Meth.* **594** (2008) 140.

[5] L. Benussi et al., *Study of gas purifiers for the CMS RPC detector*, *Nucl. Instrum. Meth.* **661** (2011) 241 [arXiv:1012.5511].

[6] V.P. Chviruk, O.V. Linuycheva and E.M. Zaverach, *Galvanic-type electrochemical sensor for determining the content of hydrohalogens in the air*, *Sensors Actuator.* **B 92** (2003) 60.

[7] F. Bergera, J.B. Sancheza and O. Heintzb, *Detection of hydrogen fluoride using SnO_2-based gas sensors: understanding of the reactional mechanism*, *Sensors Actuator.* **B 143** (2009) 152.

[8] S. Kaciulis et al., *Investigation of thin films of mixed oxides for gas-sensing applications*, *Surf. Interface Anal.* **34** (2002) 672.

[9] Y. Suna, L. Chena, F. Zhangb, D. Li, H. Pana and J. Yec, *First-principles studies of HF molecule adsorption on intrinsic graphene and Al-doped graphene*, *Solid State Commun.* **150** (2010) 1906.

[10] J.A. Buck, *Fundamentals of optical fibers*, 2nd edition, Wiley and Sons, Inc., New York U.S.A. (2004).

[11] J. Zubia and J. Arrue, *Plastic optical fibers: an introduction to their technological processes and application*, *Opt. Fiber Technol.* **7** (2001) 101.

[12] U. Steiger, *Sensor properties and applications of POFs*, in proceedings of 7th *International Conference on Plastic Optical Fibres and Applications (POF98)*, October 5–8, Berlin, Germany (1998).

[13] G. Durana et al., *Use of a novel fiber optical strain sensor for monitoring the vertical deflection of an aircraft flap*, *IEEE Sensors J.* **9** (2009) 1219.

2012 JINST 7 P12006

[14] S. Corbellini et al., *Modified POF sensor for gaseous hydrogen fluoride monitoring in the presence of ionizing radiations*, *IEEE Trans. Instrum. Meas.* **61** (2012) 1201.

[15] O. Ziemann et al., *POF Handbook — Optical short range transmission systems*, 2nd edition, Springer, U.S.A. (2008).

[16] B. Ruchti et al., *Development of new scintillating fiber detectors for high energy physics applications*, *IEEE Trans. Nucl. Sci.* **36** (1989) 146.

[17] G. Perrone and A. Vallan, *A low-cost optical sensor for non contact vibration measurements*, *IEEE Trans. Instrum. Meas.* **58** (2009) 1650.

[18] E. Angelini et al., *Plastic optic fiber sensor for cumulative measurements* in the proceeding of the *International Conference on Instrumentation and Measurements (I2MTC2009)*, May 5–7, Singapore (2009).

[19] R.H. West and S. Dowling, *Measurement of long term, radiation induced losses in fibre optics using optical time domain reflectometry*, *IEEE Trans. Nucl. Sci.* **39** (1992) 418.

[20] H. Liu, D.W. Miller and J. Talnagi, *Gamma radiation resistant Fabry-Perot fiber optic sensors*, *Rev. Sci. Instrum.* **73** (2002) 3112.

[21] W.H. Hardwick and A.H. Kalma, *Effects of low-dose-rate radiation on opto-electronic components and the consequences upon fiber optic data link performance*, *IEEE Trans. Nucl. Sci.* **26** (1979) 4808.

[22] B. Chiron, *The behaviour of POF under nuclear radiation: applications for nuclear detector scintillators, data transmission & illumination*, *IEE Colloq. Plast. Mater. Opt. Trans.* **5** (1989) 1.

[23] C. Antoine, *Tensions des vapeurs; nouvelle relation entre les tensions et les tempè*, *Compt. Rend. Acad. Sci.* **107** (1888).

[24] http://webbook.nist.gov/chemistry/, (Sept. 2011).

[25] *Hydrofluoric acid properties*, available at http://honeywell.com, (Sept. 2011).

[26] M. Tomozawa and T. Takamoriz, *Relation of surface structure of glass to HF acid attack and stress state*, *J. Amer. Ceram. Soc.* **62** (1979) 370.

2012 JINST 7 P12006